Macromolecules

pubs.acs.org/Macromolecules Article

The Hofmeister Effect on Agar Hydrogels with Mechanical Tunability and Molecular Mechanism

Jueying Yang, Weiting Huang, Jingyu Deng, Jian Li, Shahrudin Ibrahim, Younghwan Choe, Chang Su Lim, Lijie Li, Yu Chen,* and Nam-Joon Cho*

Cite This: *Macromolecules* 2026, 59, 1416−1428 Read Online

ACCESS | Metrics & More | Article Recommendations | Supporting Information

ABSTRACT: Owing to their biocompatibility and thermal responsiveness, Agar hydrogels are extensively applied in chemistry and biology fields. However, their fixed water content and rigid sugar ring structure normally exhibit limited mechanical strength, while introducing additional networks possibly deteriorates the intrinsic thermoreversible cross-linking properties of Agar hydrogel. In this work, we achieve the mechanical enhancement and tunability of Agar-based single-network hydrogels based on the Hofmeister effect via a preforming postimmersion method without the need for supplementary networks. After being immersed in different solutions of the Hofmeister salt series, the tensile strength and toughness of Agar hydrogels can be regulated between 54.7−412.1 kPa and 5.5−94.1 kJ m^{-3}. Macroscopic and microscopic analyses via SEM and SAXS, together with molecular dynamics simulations, were employed to reveal the systematic mechanisms from the number of hydrogen bonds to the aggregation state and ultimately to the mechanical properties. Since the gelation of Agar relies on double-helix formation, the Hofmeister series and regulation behaviors are different from typical synthetic polymer hydrogels. These results further promoted the elucidation of the water state regulation in the hydration layer of Agar hydrogels. This work provides an understanding of the correlation between the cross-linking state of molecular chains and the resultant Agar hydrogel properties based on the Hofmeister effect, which inspires research on the mechanical regulation mechanisms of natural polysaccharide-based hydrogels.

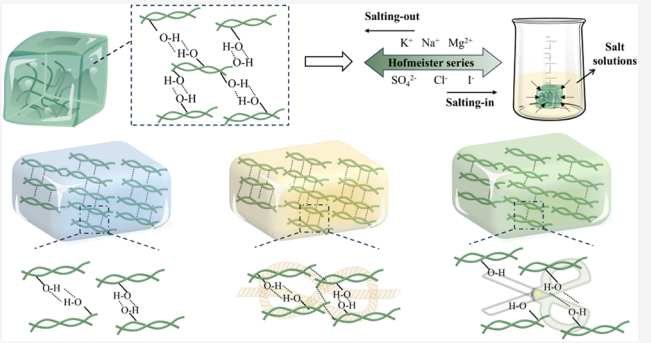

INTRODUCTION

As one of the most important natural polysaccharides, Agar is extracted from red seaweeds and serves as an eco-friendly renewable alternative to traditional synthetic polymers in alignment with sustainable development principles.[1−3] The linear polymer chain in the structure of Agar is composed of disaccharide repeating units of (1,3)-β-d-galactose and (1,4)-3,6-anhydro-α-l-galactose,[4] which can form a three-dimensional double-helix formation through hydrogen bonding, endowing Agar-based hydrogels with remarkable intrinsic thermoreversible cross-linking characteristics without toxic cross-linking agents and catalysts.[5] Although Agar hydrogels are extensively applied in medical treatment,[6] wearable sensing,[7] and sports rehabilitation,[8] they exhibit weak mechanical strength and nonadjustable properties due to a high water content exceeding 90% and a rigid sugar ring structure in the polymer chain.[9]

The current approach to improving the mechanical properties of Agar-based polymers generally involves introducing other types of polymers to the physically cross-linked Agar hydrogel networks, including poly(vinyl alcohol) (PVA),[10] polyacrylamide (PAM),[2] and gelatin (Gela).[11] However, the interactions between these polymers and Agar molecular chains can partially undermine the thermal responsiveness properties of Agar hydrogels.[12] In addition, it is challenging to regulate the properties under identical water content and polymer ratio, especially after the Agar hydrogels are prepared via the sol−gel transition process. Therefore, improving and tuning the properties of Agar-based single-network hydrogels without introducing additional networks is crucial for investigating the relationship between the cross-linking state of molecular chains and the resulting material properties in these hydrogels.

Previous studies have demonstrated that salt ions can be employed to modulate the precipitation of proteins, which is known as the Hofmeister effect.[9,13,14] This phenomenon is driven by the interaction between proteins and the surface

Received: November 14, 2025
Revised: January 9, 2026
Accepted: January 14, 2026
Published: January 26, 2026

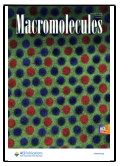

https://doi.org/10.1021/acs.macromol.5c03189
Macromolecules 2026, 59, 1416−1428

hydration layer influenced by salt ions, leading to their folding and subsequent precipitation.[15] Based on the Hofmeister effect, recent research has reported the regulation of the mechanical strength, hydrophilicity, and hydrophobicity of gelatin or polypeptide hydrogels via this mechanism.[16] Similar to protein-based materials, studies have demonstrated that polymer hydrogels, especially PVA hydrogels and poly(methacrylamide) (PMAm), can also demonstrate the Hofmeister effect, which has been applied to improve mechanical properties,[17,18] antifreeze hydrogel electrolytes,[19] solar-driven water evaporation devices,[20] wearable conductive devices,[21,22] and actuators.[23] Inspired by the mechanical improvement of natural protein, PVA, and PMAm hydrogels, it can be proposed that the properties of natural polysaccharide single-network hydrogels, such as Agar hydrogels, can also be regulated through the Hofmeister effect. However, the research on these kinds of polymers and their systematic mechanism from the microscopic to the macroscopic level remains largely unexplored. Since the gelation of Agar hydrogels relies on double-helix formation, the manifestation of the Hofmeister effect in these hydrogels cannot be directly inferred from other systems.

In this work, we analyzed the Hofmeister effect on Agar-based single-network hydrogels with mechanical tunability and molecular mechanisms. Agar hydrogels were prepared via the preforming postimmersion methods, allowing for the mechanical properties of the Agar hydrogels to be tuned by the Hofmeister effect. The microstructure of Agar hydrogels was investigated under the Hofmeister salt series. The mechanism underlying the mechanical tunability was also explored using molecular dynamics simulations. The water state regulation of Agar hydrogels by immersing them in different types of salt solutions further proved the microstructural characterizations and mechanism analysis of the Hofmeister effect. These findings provide a valuable reference for tuning the properties of other natural polysaccharide polymer hydrogels based on the molecular mechanism of the Hofmeister effect.

EXPERIMENTAL SECTION

Materials

Agar (reagent grade; gel strength of a 1.5% gel is 1638 g cm^{-2}), potassium chloride (KCl), sodium chloride (NaCl), lithium chloride (LiCl), calcium chloride ($CaCl_2$), magnesium chloride ($MgCl_2$), sodium sulfate (Na_2SO_4), sodium carbonate (Na_2CO_3), sodium acetate (NaAc), and sodium iodide (NaI) were all purchased from Sigma-Aldrich Merck Co., Ltd.

Preparation of Agar Hydrogel

Agar hydrogel was prepared by the preforming postimmersion method. First, 0.6 g of Agar powder was added to a flat-bottom flask containing 20 mL of deionized water. The mixed liquid containing Agar powders was heated to 100 °C under magnetic stirring until it was completely boiled to form an Agar sol. Subsequently, the Agar sol was stirred continuously until it was maintained at 80 °C, kept warm for 5 min, and poured into a mold after the bubbles disappeared. After cooling at room temperature (25 °C) for 30 min, the Agar sol was slowly cross-linked to obtain the preformed hydrogel via a sol−gel transition. The preformed Agar hydrogel was entirely peeled from the mold and placed in a 20 mL salt solution with a concentration of 1 mol L^{-1} or 20 mL deionized water. After immersion at room temperature for 24 h, it was taken out and the surface salts were rinsed with deionized water three times. Among them, the salt solution includes KCl, NaCl, LiCl, $CaCl_2$, $MgCl_2$, Na_2SO_4, Na_2CO_3, NaAc, and NaI solution. Agar hydrogels immersed in deionized water, Na_2SO_4, NaCl, and NaI solutions were named Agar/H_2O hydrogel, Agar/SO_4^{2-} hydrogel, Agar/Cl^- hydrogel, and Agar/I^- hydrogel, respectively. To compare the preforming post-immersion method and the one-pot direct adding method, the control group of Agar hydrogels was prepared using the one-pot direct adding method. Specifically, the Agar sol was obtained by heating the Agar powders until they were completely dissolved in water. Subsequently, Na_2SO_4 powders were added to the Agar sol and stirred continuously until the salt powders were completely dissolved. The sol was kept warm for 5 min and poured into a mold after the bubbles disappeared. After cooling at room temperature for 30 min, the Agar sol containing SO_4^{2-} was slowly cross-linked to obtain the hydrogel via a sol−gel transition. The thermoreversible cross-linking properties of Agar hydrogels before and after salt treatment were verified by the macroscopic appearance of the Agar/H_2O and Agar/Na_2SO_4 hydrogels before and after being mechanically disrupted, heated to the sol state, and subsequently cooled to form gels again via the sol−gel transition.

Mechanical Tests

The mechanical properties of Agar hydrogel were characterized by a universal mechanical testing machine. For the tensile test, the samples were cut using a dumbbell-shaped die, the size of the effective fracture area was kept at 4 mm × 20 mm, the tensile rate was set to 100 mm min^{-1}, and the samples were stretched until they broke. For the compression test, the samples were cut using a cylindrical die, the size of the effective fracture area was kept at 10 mm in diameter, the compression rate was set to 2 mm min^{-1}, and the samples were compressed until they broke. Young's modulus was calculated by the ratio of stress and strain of the sample in the elastic deformation stage, and the toughness was calculated by the integral area of the stress and strain curve of the sample before fracture. Three groups of each sample were tested and the average value was taken. To verify the reversible cross-linking behaviors of the hydrogels, the tensile tests were performed on Agar/Na_2SO_4 hydrogels sequentially immersed in 1 mol L^{-1} Na_2SO_4 solution, H_2O, and then again in 1 mol L^{-1} Na_2SO_4 solution.

Rheology Tests

The dynamic rheological properties of Agar hydrogel after immersion in different solutions were characterized by a rotational rheometer. The sample was cut into thin slices with a diameter of 25 mm, and a parallel plate rotor with a diameter of 25 mm was selected for testing. The plate temperature was set to 25 °C, the strain was 0.5%, the scanning angular frequency was 1−100 rad s^{-1}, and the storage modulus (G') and loss modulus (G'') of the sample were recorded. The loss tangent value, average grid size, and cross-linking density can be calculated based on the G' and G'' at the angular frequency of 10 rad s^{-1} according to the rubber elasticity theory by the following equations:[24]

$$\tan\delta = \frac{G''}{G'} \tag{1}$$

$$\xi = \left(\frac{G' N_A}{RT}\right)^{-1/3} \tag{2}$$

$$n_c = \frac{G_e}{RT} \tag{3}$$

where $\tan\delta$ is the loss tangent value, ξ is the average grid size, N_A is the Avogadro constant (6.02×10^{23}), R is the gas constant (8.314 J K^{-1} mol^{-1}), and T is the test temperature (298 K), n_c is the cross-linking density of the hydrogel, and G_e is the platform value of the storage modulus measured by frequency scanning of the hydrogel.

Scanning Electron Microscopy

The microstructures of Agar hydrogel were characterized by field emission scanning electron microscopy (SEM). After the samples were fractured with liquid nitrogen and freeze-dried, they were pasted on the surface of conductive glue with the cross-section facing up, and

https://doi.org/10.1021/acs.macromol.5c03189
Macromolecules 2026, 59, 1416−1428

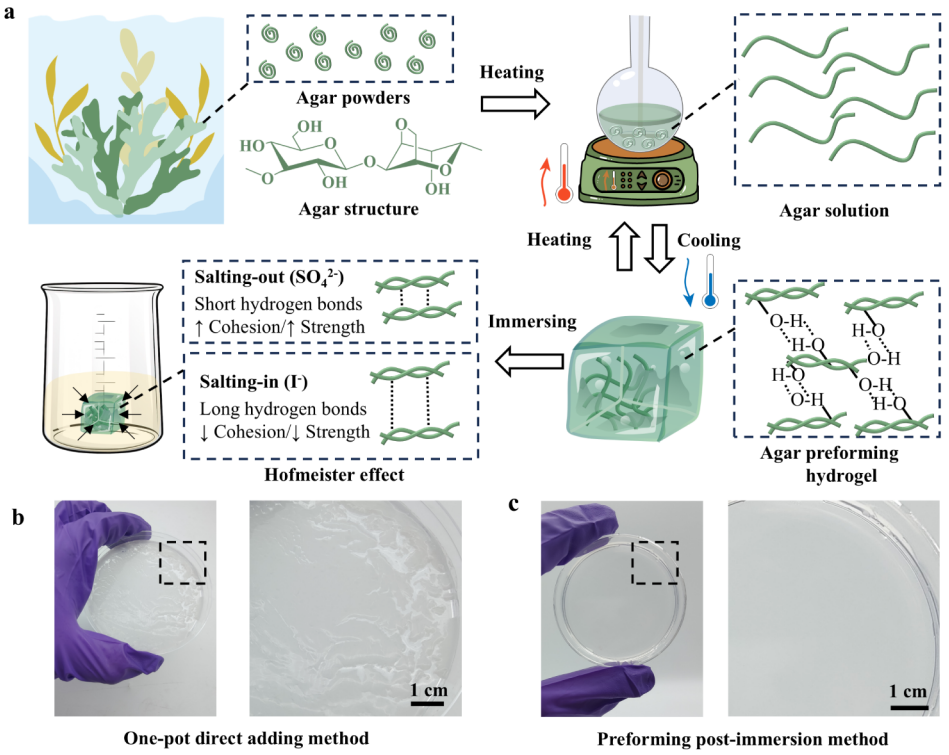

Figure 1. Schematic diagram of the preparation and formation mechanism of Agar hydrogel. (a) Preparation process of Agar hydrogel; (b-c) Images of Agar/SO_4^{2-} hydrogel prepared by one-pot direct adding method (b) and preforming postimmersion method (c).

the samples were sprayed with gold. The acceleration voltage was set to 5 kV during observation.

Small-Angle X-ray Scattering

The nanostructures of the Agar hydrogels were characterized by small-angle X-ray scattering (SAXS). SAXS experiments were performed on a X-ray scattering instrument equipped with a Cu Kα radiation source (λ = 0.154 nm). The sample-to-detector distance was adjusted to cover a q range of 0.074−2.5 Å^{-1}. The exposure time for each sample was 300 s. The SAXS profiles were further analyzed and fitted using the mass-fractal model.

Fourier Transform Infrared Spectroscopy

The chemical structures of Agar hydrogels were tested by the Attenuated Total Reflection Fourier transform infrared (ATR-FTIR) spectroscopy. To avoid the interference of water content in the hydrogel, freeze-dried hydrogel samples were used for testing, and the spectral scanning range was set to 4000−600 cm^{-1} with a resolution of 4 cm^{-1}.

Differential Scanning Calorimetry

Differential scanning calorimetry (DSC) was used to characterize the state of water molecules in the hydration layer of Agar hydrogels immersed in different solutions. The heating rate was set to 10 °C min^{-1}, the nitrogen flow rate was 50 mL min^{-1}, the temperature scanning range was −30 to 30 °C, and the DSC curve of the sample was peak-fitted using Systat PeakFit software. The melting enthalpy $\Delta H(T)$ of water in the hydrogel can be calculated according to eq 4:[20]

$$\Delta H(T) = \Delta H(273) - \int_T^{273} \Delta C_p dt \tag{4}$$

where $\Delta H(273)$ is the melting enthalpy of H_2O (334 J g^{-1}), T is the melting temperature of supercooled water, and ΔC_p is the heat capacity difference between intermediate water and ice. eq 4 can be further simplified to eq 5:

$$\Delta H(T) = \Delta H(273) + 2.119 \times \Delta T - 0.00783 \times \Delta T^2 \tag{5}$$

wherein, ΔT is the difference between the melting temperature of supercooled water and the melting temperature of H_2O (273 K). Therefore, the contents of intermediate water, free water, and bound water can be calculated according to eq 6:

$$\omega_{IW} = {\Delta H_{IW}}^{exp} / \Delta H(T) \tag{6}$$

$$\omega_{FW} = {\Delta H_{FW}}^{exp} / \Delta H(T) \tag{7}$$

$$\omega_{BW} = 1 - \omega_{IW} - \omega_{FW} \tag{8}$$

wherein, ω_{IW}, ω_{FW}, ω_{BW} are the contents of intermediate water, free water, and bound water, respectively, and ${\Delta H_{IW}}^{exp}$, ${\Delta H_{FW}}^{exp}$ are the melting enthalpies of intermediate water and free water, respectively, which can be obtained by integrating the areas of intermediate water and free water after peak fitting of the DSC curve.[20]

Confocal Raman Spectroscopy

Confocal Raman spectroscopy (Raman) was used to characterize the state of water molecules in the hydration layer of Agar hydrogels immersed in different solutions. The scanning range was set to 3000−4000 cm^{-1}, the resolution was set to 4 cm^{-1}, the laser wavelength was set to 488 nm, and the Raman spectrum curve was fitted with the Systat PeakFit software.

Molecular Dynamics Simulation

To explore the mechanism of the Hofmeister effect, the molecular dynamics simulation in Materials Studio (MS) software was used to calculate the radial distribution function (RDF) and hydrogen bond number between H atoms and O atoms that may produce hydrogen bonds in the Agar molecular chain in H_2O, Na_2SO_4, NaCl, and NaI salt solutions. The detailed steps are provided in the Supporting Information.

RESULTS AND DISCUSSION

In this work, a preforming postimmersion method was employed to fabricate Agar-based single-network hydrogels,

https://doi.org/10.1021/acs.macromol.5c03189
Macromolecules 2026, 59, 1416−1428

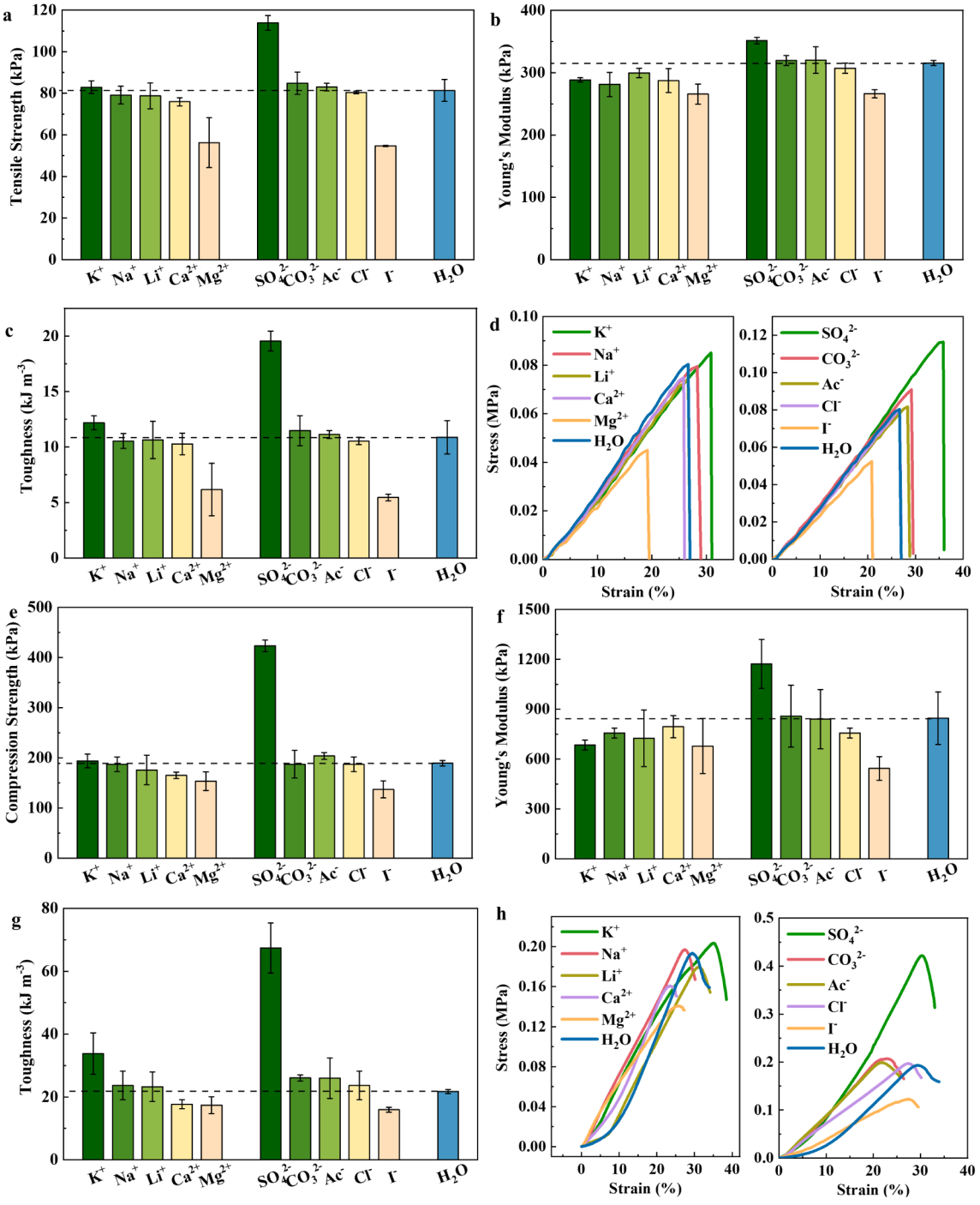

Figure 2. Mechanical test results of Agar hydrogels immersed in different ionic solutions with a concentration of 1 mol L^{-1}. (a) Maximum tensile strength; (b) Tensile Young's modulus; (c) Tensile toughness; (d) Tensile curve; (e) Maximum compressive strength; (f) Compressive Young's modulus; (g) Compressive toughness; (h) Compression curve. The data were presented as mean value ± standard deviation.

which were subsequently exposed to various salt solutions to induce interactions. The preparation scheme is shown in Figure 1a. Preformed Agar hydrogels were obtained owing to the unique thermoreversible sol−gel transition of Agar. The hydrogen bonds between Agar polymer chains can be broken under continuous heating to dissolve Agar powders and form a uniformly flowing liquid phase at high temperatures (100 °C).[25] During the cooling process at room temperature (25 °C), the hydrogen bonds between Agar polymer chains will reassociate and form a cross-linked hydrogel structure.[12] Since the interaction between hydrogen bonds constitutes a reversible physical cross-linking, the sol−gel transition of Agar hydrogel is also reversible, thereby conferring a distinctive molding advantage to the material.[8] The Agar hydrogels regulated by different types of salts were prepared by the following immersion of preformed Agar hydrogels in various salt solutions, which was used for the further analysis of the Hofmeister effect. Hydrogels immersed in deionized water, Na_2SO_4, NaCl, and NaI solutions were named as Agar/H_2O hydrogel, Agar/SO_4^{2-} hydrogel, Agar/Cl^- hydrogel, and Agar/I^- hydrogel, respectively. As the system contains only the Agar-based cross-linking network, it provides a superior model for

https://doi.org/10.1021/acs.macromol.5c03189
Macromolecules 2026, 59, 1416−1428

exploring the relationship between the properties of tunability and the molecular mechanisms involved in single-network polysaccharide hydrogels through the regulation of salt ions.

In previous studies, the Hofmeister effect has been investigated by immersing samples in salt solutions. Taking Agar/SO_4^{2-} hydrogel as an example, to analyze the necessity of the immersing step and the functionality of the preforming postimmersion method for the preparation of uniform and robust Agar hydrogel samples, a comparative hydrogel was prepared using the one-pot direct adding method by directly adding Na_2SO_4 powders to the Agar sol, followed by the cooling process at room temperature. The appearances of the Agar/SO_4^{2-} hydrogel prepared by the preforming post-immersion method and one-pot direct adding method are shown in Figure 1b. The one-pot direct adding method leads to an incomplete formation of the Agar/SO_4^{2-} hydrogel, which manifests as a fragmented and structurally compromised network, and its mechanical strength cannot be measured. In contrast, the Agar/SO_4^{2-} hydrogel prepared via the preforming postimmersion method presents a uniform and intact hydrogel structure that can be fully detached from the mold, demonstrating superior mechanical integrity. The difference between the two preparation methods could be attributed to the tendency of high concentrations of ions in the salt solution to disrupt the hydrogen bonding interactions among Agar molecular chains, thereby affecting the hydrogel formation process. For the hydrogel prepared by the one-pot direct adding method, the ions can influence the solvation dynamics of water molecules between Agar chains and alter the intermolecular spacing, leading to the collapse of the hydrogel structure (Figure S1).[26,27] For the hydrogel prepared by the preforming postimmersion method, since the Agar polymer chain in the preformed hydrogel is already cross-linked, the postimmersion in a Na_2SO_4 salt solution primarily affects the strength of hydrogen bonds by regulating the solvation of water around the Agar chains. This process does not significantly alter the intermolecular spacing between chains, thus preserving the integrity of the preformed cross-linked structure while allowing for further regulation of the properties. Therefore, the preforming postimmersion method is important in obtaining uniform and intact Agar hydrogels that can effectively interact with different ions. In addition, the salt treatment preserves the intrinsic thermoreversible cross-linking behavior of Agar hydrogel, as both Agar/H_2O and Agar/Na_2SO_4 hydrogels exhibit reversible sol−gel transition upon heating and cooling (Figure S2).

The macroscopic regulation of different salt solutions on the molecular chains of Agar hydrogels is manifested as differences in mechanical properties. The influence of the Hofmeister effect on the tensile properties of Agar hydrogels immersed in the Hofmeister salt series with a concentration of 1 mol L^{-1} was evaluated by uniaxial tensile tests. The results of maximum tensile strength, Young's modulus, toughness, and tensile curves are shown in Figure 2a-d.

As shown in Figure 2, the mechanical properties of Agar hydrogels are regulated after immersion in the Hofmeister salt series. For cationic salt solutions, the order of mechanical strength and toughness of Agar hydrogels is $K^+ > Na^+ \approx Li^+ > Ca^{2+} > Mg^{2+}$. Among these ions, K^+ enhances the mechanical properties of the Agar hydrogel, while Na^+, Li^+, and Ca^{2+} have little effect on its mechanical properties. In contrast, Mg^{2+} significantly decreases the mechanical strength and toughness of Agar hydrogel, reducing the mechanical strength from 81.4 to 56.2 kPa and toughness from 10.9 kJ m^{-3} to 6.2 kJ m^{-3}. For anionic solutions, the order of mechanical strength and toughness of Agar hydrogels is $SO_4^{2-} > CO_3^{2-} \approx Ac^- > Cl^- > I^-$. Among them, the Agar/$SO_4^{2-}$hydrogel exhibits the highest strength (113.9 kPa), elongation (35.8%), and toughness (19.6 kJ m^{-3}). CO_3^{2-}, Ac^-, and Cl^- have minimal impact on the mechanical properties, while the hydrogel immersed in I^- has the lowest strength (54.7 kPa), elongation (20.8%), and toughness (5.5 kJ m^{-3}), with the toughness being only 50% of that of the Agar hydrogel immersed in H_2O. Due to the high water content, chain rigidity, and soft nature of Agar hydrogels, the samples fractured at relatively small tensile strains, as shown in Figure 2d. Furthermore, as the concentration of SO_4^{2-} solution increases, the mechanical properties of the hydrogel are further enhanced, reaching 412.1 kPa and 94.1 kJ m^{-3} at the concentration of 2 mol L^{-1}, which is 7.5-fold and 17.1-fold higher than that of the Agar/I^- hydrogel (Figure S3). This demonstrates that anions have a greater effect on the mechanical properties of Agar hydrogel than cations due to the stronger interaction between anions and the hydration layer on the surface of the polymer, which is consistent with the phenomenon observed in proteins and some synthetic polymers by the Hofmeister effect.[13,28]

To further assess the impact of the Hofmeister effect on the compression properties, uniaxial compression tests were conducted on Agar hydrogels immersed in H_2O and different salt solutions. The maximum compression strength, Young's modulus, toughness, and compression curve are shown in Figure 2e-h. The compression properties of Agar hydrogels in different salt solutions followed a similar trend to that observed in the tensile properties. Due to the Hofmeister effect, Agar/SO_4^{2-} hydrogel shows the highest compressive strength, with a toughness that is 3.1 times greater than that of the Agar/H_2O hydrogel, while Agar/I^- hydrogel exhibits the lowest compressive strength, with a toughness that is only 73.3% of the Agar/H_2O hydrogel. The compression test results verify that the compression properties of the Agar hydrogel can be regulated by the Hofmeister effect, with compressive strength and toughness tunable within the ranges of 137.2−423.6 kPa and 15.9−67.4 kJ m^{-3}, respectively.

These experimental results confirm the initial hypothesis that the salt series in the Hofmeister effect can effectively regulate the mechanical properties of polysaccharide-based hydrogels like Agar. Notably, the tensile and compression toughness of the Agar hydrogel can be tuned by more than an order of magnitude.[29] However, compared to synthetic polymer hydrogels, such as PVA, which has been extensively studied, the mechanical properties of Agar hydrogels are less significantly affected by the concentrations of salts.[13,14,30] This difference may be attributed to the interaction of hydrogen bonds in the hydration layer and the hydrophobic properties of the hydrogel structure. On the one hand, synthetic polymers such as PVA have long carbon chain skeletons. This flexible structure makes it easier for ions to interact with hydration layer molecules, thereby affecting the hydrogen bonds between PVA molecular chains and water molecules. On the other hand, ions can alter the hydrophobic hydration of molecules by raising the surface tension within the cavities around the PVA chains. In contrast, the rigid sugar-ring structure and the double-helix formation of Agar hydrogels restrict chain flexibility, which also provides abundant hydroxyl groups for hydrogen bonding with water molecules. Consequently, salt ions regulate the chain structure primarily through interactions

https://doi.org/10.1021/acs.macromol.5c03189
Macromolecules 2026, 59, 1416−1428

with the hydration layer molecules surrounding the polar functional groups, rather than through direct interaction with the polymer chains. However, the mechanical properties regulation of Agar hydrogels via the Hofmeister effect demonstrates considerable practical value. This approach enables the precise tuning of the mechanical properties of Agar hydrogels without necessitating the incorporation of additional network structures, while also allowing for accessible postsynthesis adjustability. As shown in Table 1, in comparison to other methods for regulating the mechanical properties of Agar hydrogels, such as the incorporation of double networks or variations in composition,[6,7,12,31−33] the Hofmeister effect offers a facile and broadest range of tunability (up to 7.5 times), thereby enhancing their potential for diverse applications.

Table 1. Comparison of Agar Hydrogels Regulated by the Hofmeister Effect and Other Hydrogels

Materials	Mechanical regulation	Tunability after preparation	Mechanical strength
κ-carrageenan and agar hydrogel[6]	No	No	47.8 kPa
Agar/polyacrylamide hydrogel[31]	No	No	∼17 kPa
PVA−agar hydrogel[32]	Double network	No	43−149 kPa
Agar/Borax/MXene hydrogel[7]	Different pH	No	∼40−225 kPa
Agar/κ-carrageenan/montmorillonite hydrogel[33]	Different composition	No	33.8−47.7 kPa
Agar/poly(sulfobetaine methacrylate) hydrogel[12]	Double network and mechanical pressing	Yes	6.5−78.1 kPa
Agar hydrogel (This work)	Hofmeister effect	Yes	54.7−412.1 kPa

The mechanical properties of the material are related to the cross-linking state of the molecular chain. Therefore, the rheological properties of Agar hydrogels were characterized, and the results are shown in Figure 3a-b. For all hydrogels, in the angular frequency range of 1−100 rad s^{-1}, the storage modulus (G') is higher than the loss modulus (G'') and these two lines are nearly parallel, indicating that the elastic response of the hydrogel is predominant over the viscous response. The ratio of G'' to G' ($\tan\delta$) of all of the Agar hydrogels is less than 0.1, indicating that the Agar hydrogel is stable and exhibits low viscous dissipation and predominantly elastic behaviors (Figure S4).[8] The average mesh size (ξ) and cross-link density (n_c) between adjacent cross-linking points of the Agar hydrogel in the equilibrium state with an angular frequency of 10 rad s^{-1} were calculated using eqs 2 and 3, as shown in Figure 3c-d. The ξ of the hydrogel varies from 4.7 to 5.7 nm, while the n_c varies from 8.7 mol m^{-3} to 16.2 mol m^{-3}. This supports the hypothesis that during the immersion process, ions in the Hofmeister salt series mainly impact the aggregation state of the Agar polymer chains.[18,24] Under the influence of the Hofmeister effect, Agar hydrogels immersed in ions that induce a "salting-out" effect (such as K^+, SO_4^{2-}) exhibit higher G' and n_c values, and lower ξ value compared to the hydrogels immersed in H_2O. In contrast, Agar hydrogels immersed in ions that induce a "salting-in" effect (such as Mg^{2+}, I^-) exhibit lower G' and n_c values, and higher ξ value compared to the hydrogels immersed in H_2O. The differences among cations of the same group and valence arise from their distinct capacities to modulate the structure of the hydration shell, which may be associated with variations in their ionic radii. The variations in ξ and n_c among different ions are generally consistent with the mechanical performance, following the Hofmeister series. Small deviations arise from the fact that ξ and n_c values are derived from equilibrium swelling theory, which primarily reflects thermodynamic network constraints, whereas tensile strength and toughness are affected by multiple coupled

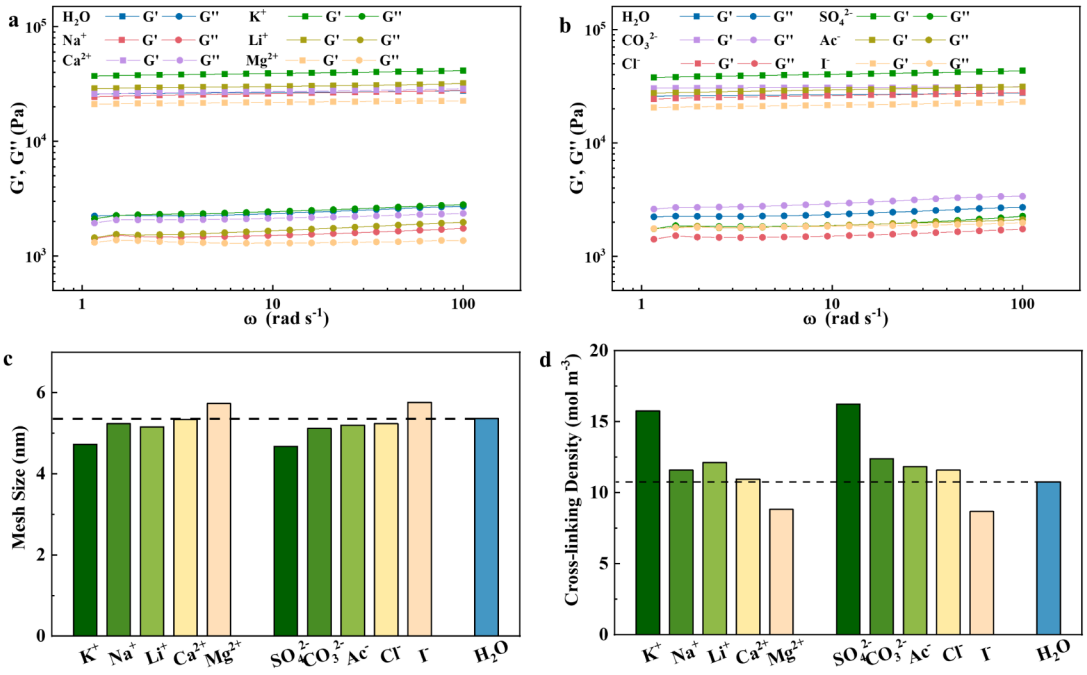

Figure 3. Rheological properties of Agar hydrogels after immersing in different salt solutions. (a-b) Frequency sweep of Agar hydrogels immersing in cationic (a) and anionic (b) solutions; (c) Mesh size of Agar hydrogels; (d) Cross-linking density of Agar hydrogels.

https://doi.org/10.1021/acs.macromol.5c03189
Macromolecules 2026, 59, 1416−1428

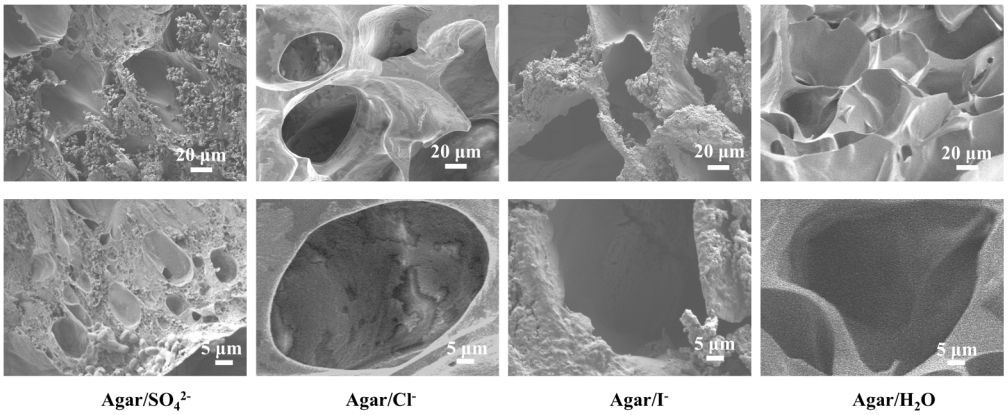

Figure 4. SEM cross-section images of Agar hydrogels after immersing in different salt solutions.

factors, including hydrogen-bond dynamics and chain orientation.[34] The viscoelastic test of Agar hydrogel further demonstrates that the aggregation state of Agar polymer chains can be regulated by ions based on the Hofmeister effect.

To characterize the microstructure changes in the aggregation state of the polymer chains in the Agar hydrogel regulated by the Hofmeister effect, the SEM cross-sectional morphology of the hydrogel was analyzed and the results are shown in Figure 4. The pore size of each of the hydrogels is shown in Figure S5. Agar/H_2O hydrogel presents a typical network-like porous structure of hydrogel with a uniform and smooth pore wall, where its pore size ranges about 56.9 ± 7.9 μm. Agar/SO_4^{2-} hydrogel shows the smallest pore structure, the highest pore density, and pore size in the range of around 10.4 ± 1.8 μm. This difference may be attributed to the "salting-out" effect, which induces the Agar polymer chains to collapse spontaneously and form a small pore structure due to dehydration.[35] The pore structure of Agar/Cl^- hydrogel is nearly identical to that of Agar/H_2O hydrogel, which may be attributed to the minimal impact of Cl^- on the aggregation state of Agar polymer chains. The pores of Agar/I^- hydrogel are significantly enlarged, with the pore size increasing to 103.6 ± 13.1 μm. In addition, the pore wall becomes rough, and some small pore structures appear on the pore walls. This phenomenon may be attributed to the "salting-in" effect of the ions, which enhances the hydration between Agar polymer chains, causing some Agar polymer chains to dissolve and thereby increasing the pore size of the hydrogel.[29]

To more direct assessment of the native hydrogel nanostructure, SAXS experiments in Agar/H_2O hydrogel and Agar/SO_4^{2-} hydrogel were conducted. For both Agar/H_2O hydrogel and Agar/SO_4^{2-} hydrogel, the SAXS profiles were fitted using the mass-fractal model (Figure S6).[36] The two samples exhibit almost identical mass-fractal dimension of 2.3, indicating that the immersing of SO_4^{2-} does not change the fundamental aggregation mode of agar chains within the hydrogel network.[25] However, the Agar/H_2O hydrogel exhibits a cutoff length (ζ) of 20.2 nm, while that of the Agar/SO_4^{2-} hydrogel decreases to 17.5 nm. The reduction in ζ indicates that the Agar/SO_4^{2-} hydrogel forms a more compact and spatially confined network structure. This structure from SAXS is consistent with the SEM observations, where the Agar/SO_4^{2-} hydrogel displays smaller pore features compared to the relatively looser network in the Agar/H_2O hydrogel.

SEM and SAXS results indicate that the "salting-out" ions promote the arrangement of polymer chains within the Agar hydrogel, leading to their aggregation and the development of a denser hydrogel network. This organization minimized the entropy loss associated with a highly ordered structure.[23] In contrast, the "salting-in" ions facilitate the dissolution of polymer chains in the Agar hydrogel, disrupting its network structure of the Agar hydrogel.

To explore the driving forces behind the changes in the aggregation state of hydrogels, ATR-FTIR tests were conducted on Agar hydrogels immersed in different salt solutions, with the corresponding results presented in Figure S7. The absorption peak at 3363 cm^{-1} in Agar hydrogel is the stretching vibration absorption peak of −OH, and the absorption peak at 1644 cm^{-1} is the stretching vibration absorption peak of C═O in agaropectin.[12] The shift in the −OH stretching vibration peak can reflect changes in hydrogen bonding interactions within the Agar hydrogel.[37] In the ion group (K^+) exhibiting a "salting-out" effect, the −OH stretching vibration peak shifts to a lower wavenumber (3335 cm^{-1}), indicating an enhancement of the hydrogen bonding between polymer chains in Agar hydrogels. Conversely, in the ion group (Ca^{2+}, Mg^{2+}, I^-) associated with a "salting-in" effect, the −OH stretching vibration peak shifts to a higher wavenumber, indicating a weakening or disruption of the hydrogen bonding within the polymer network. The hydrogen-bonding analysis mainly applies to systems containing cations and weakly absorbing anions. For samples containing strongly absorbing anions (such as Agar/SO_4^{2-}), the variations in hydrogen bonding are not directly observable from the ATR-FTIR spectra due to overlapping ionic absorption.

The combined microstructure analysis results from rheological testing, SEM imaging, SAXS analysis, and ATR-FTIR spectroscopy suggest that the Hofmeister effect may regulate the aggregation state of the Agar hydrogel by affecting the hydrogen bonding interaction between the polymer chains, thereby tuning their mechanical properties.[38] To verify this hypothesis and reveal the molecular interaction mechanisms for the regulation behaviors induced by the Hofmeister salt series, molecular dynamics simulation of Agar hydrogels immersed in typical salt solution and H_2O was performed and compared.

The molecular model construction process is shown in Figure S8. Amorphous networks of Agar/H_2O, Agar/SO_4^{2-}, Agar/Cl^-, and Agar/I^- were constructed through structural optimization followed by the annealing step, incorporating H_2O, SO_4^{2-}, Cl^- or I^- along with Agar molecular chains.

https://doi.org/10.1021/acs.macromol.5c03189
Macromolecules 2026, 59, 1416−1428

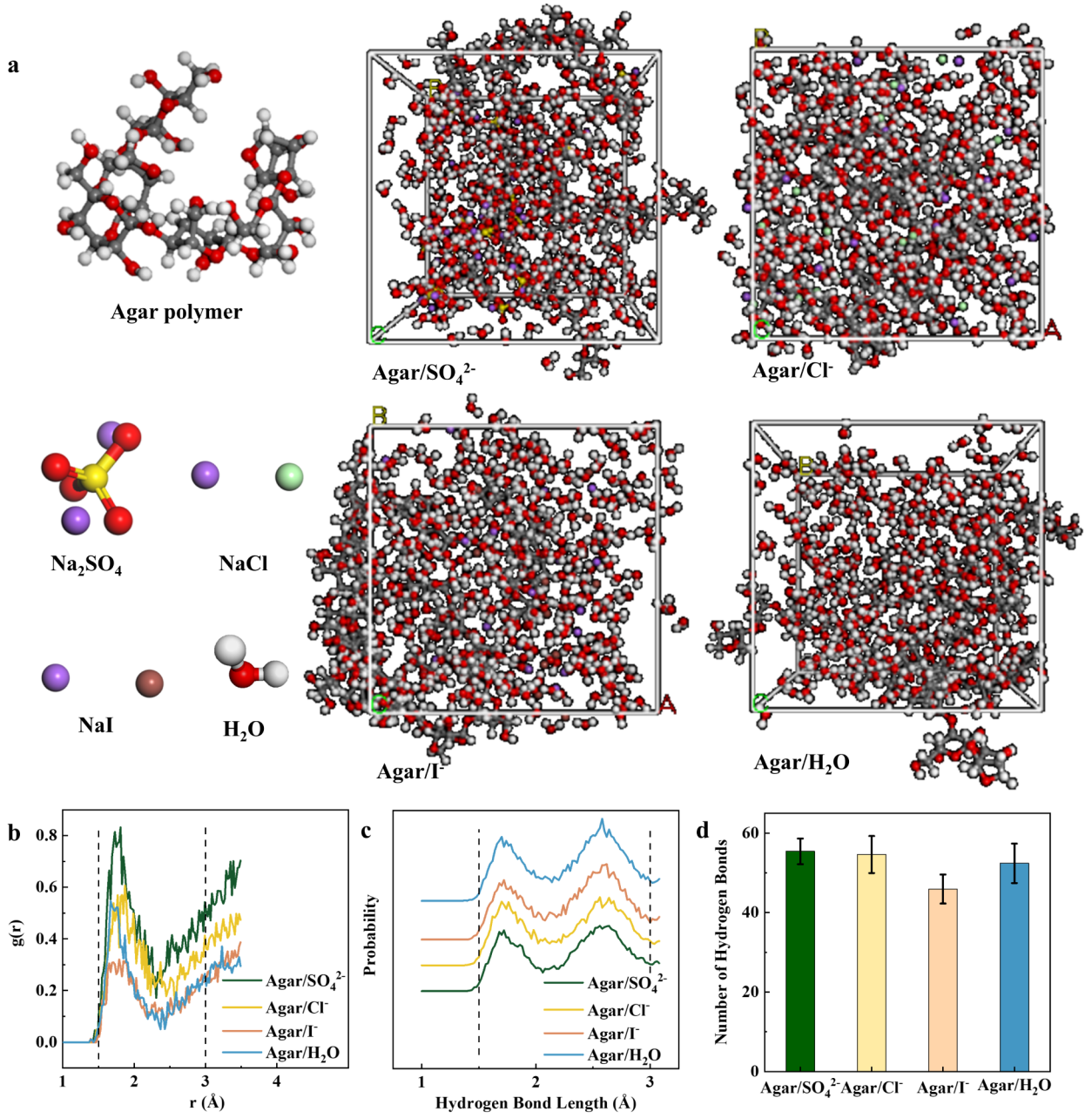

Figure 5. Molecular dynamics simulation process and results of Agar hydrogels immersed in different ion solutions. (a) Molecular dynamics simulation process; (b) Radial distribution function of H atoms and O atoms on the Agar molecular chain in different ions; (c) Probability of hydrogen bond length on the Agar molecular chain in different ions; (d) Number of hydrogen bonds on the Agar molecular chain in different ions.

Subsequently, dynamic simulations were conducted on each of these networks, and the corresponding systems containing Agar polymers and associated ions are presented in Figure 5a. The radial distribution function (RDF), the probability distribution function, and the average number of hydrogen bonds were calculated based on the dynamic simulation results (Figure 5b). The range of 1.5−3 Å in the RDF can be regarded as hydrogen bond interactions.[39] Distinct peaks within this range in the Agar/H_2O, Agar/SO_4^{2-}, Agar/Cl^-, and Agar/I^- amorphous indicate the presence of hydrogen bond interactions within each of these four network systems.[40] In addition, the probability distribution function and the average number of hydrogen bonds on the Agar polymer chain during the dynamics simulation can be calculated, and the results are shown in Figure 5c-d. Two characteristic hydrogen-bond lengths are identified at approximately 1.7 Å and 2.6 Å, corresponding to different hydrogen-bonding configurations between Agar polymer chains. A shorter hydrogen-bond length and a higher number of hydrogen bonds indicate stronger hydrogen-bonding interactions within the Agar network. It can be seen that the probability distribution intensity of the Agar/SO_4^{2-} network at 1.7 Å is similar to that at 2.6 Å, while this value of the Agar/I^- network at 1.7 Å is much smaller than that at 2.6 Å, indicating that the hydrogen bond length in the Agar/SO_4^{2-} network is shorter and the energy is higher compared to the Agar/I^- network. The Agar/Cl^- network and the Agar/H_2O network have similar hydrogen bond probability distribution functions. The comparison of the probability distribution function and the number of hydrogen bonds across different salt solutions indicates that the Hofmeister

https://doi.org/10.1021/acs.macromol.5c03189
Macromolecules 2026, 59, 1416−1428

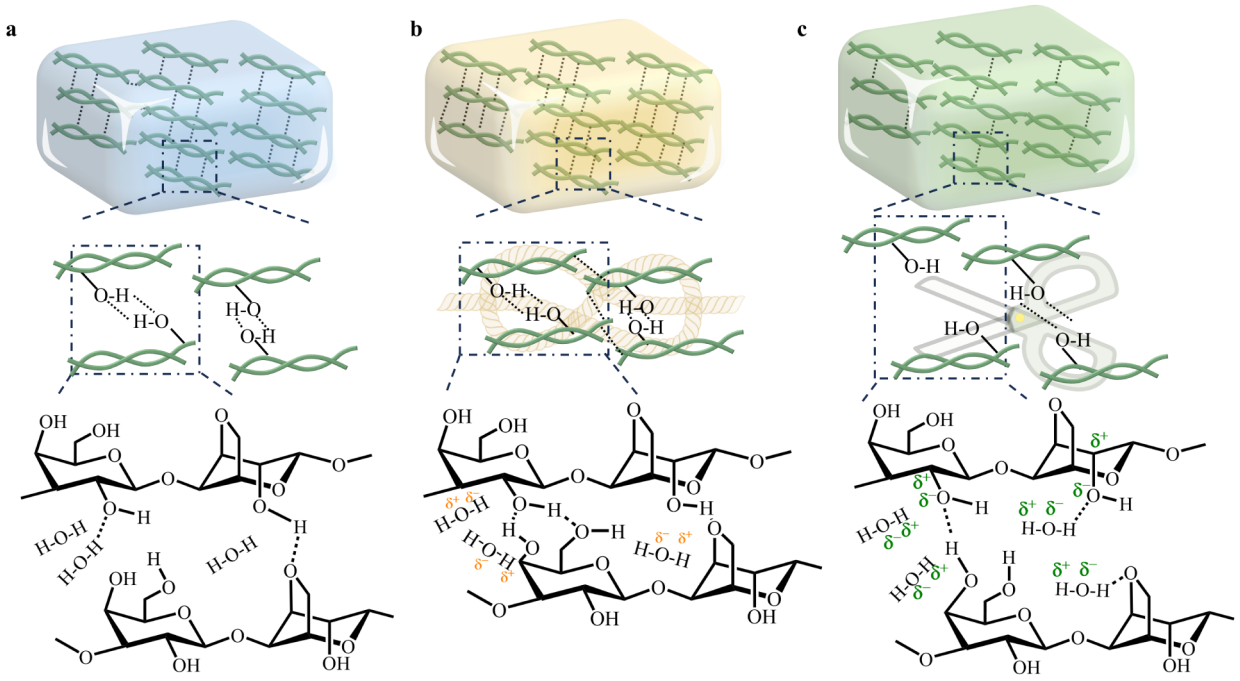

Figure 6. Schematic diagram of the Hofmeister effect mechanism of Agar hydrogels immersed in different ionic solutions. (a) The structure of Agar hydrogel in H_2O; (b) The structure of Agar hydrogel in ions with "salting-out" effect; (c) The structure of Agar hydrogel in ions with "salting-in" effect.

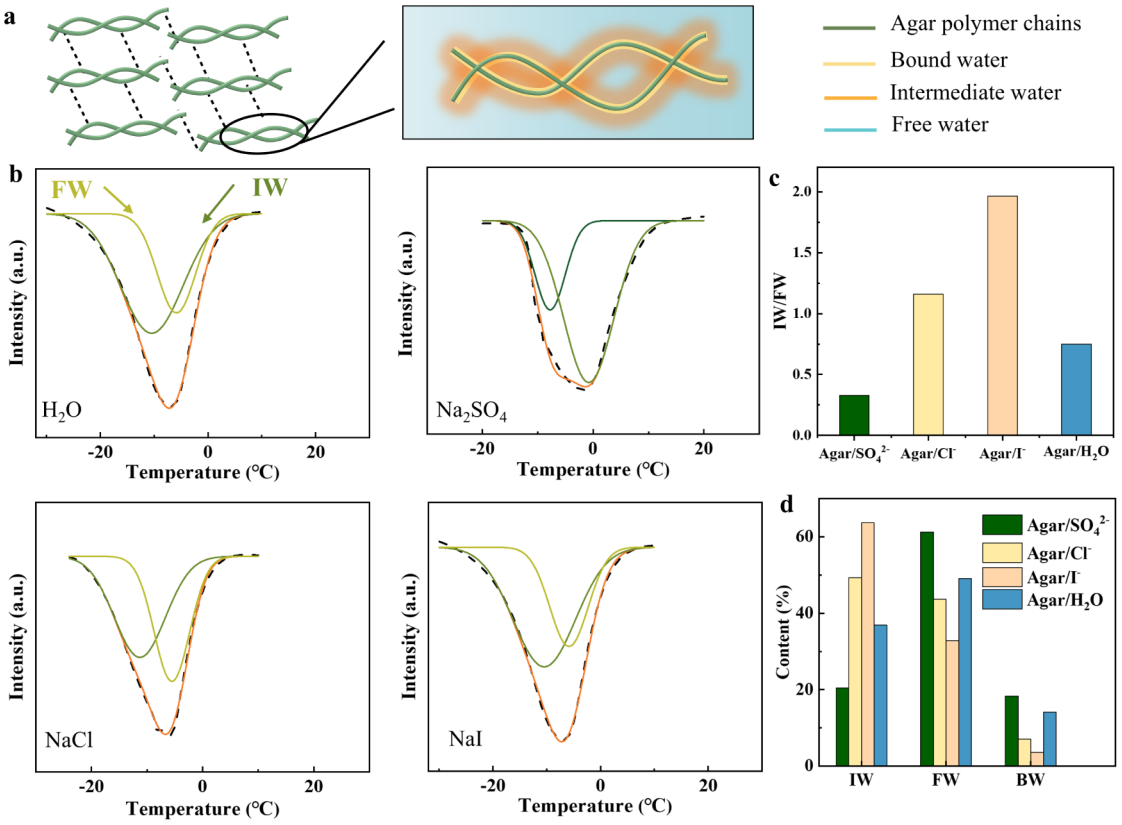

Figure 7. Water states and DSC spectroscopy characterization of Agar hydrogels immersed in different ionic solutions. (a) Schematic diagram of the network structure and water state in the Agar hydrogel; (b) DSC spectra of Agar/H_2O, Agar/SO_4^{2-}, Agar/Cl^-, and Agar/I^- hydrogels after Gaussian fitting; (c) IW/FW ratio; (d) The content of different water states.

effect can influence the formation of hydrogen bonds within the Agar networks.[41] The number of hydrogen bonds in different networks also follows the sequence observed in the Hofmeister salt series from the mechanical experiments, that is $SO_4^{2-} > Cl^- > I^-$. Therefore, the regulation of the Hofmeister effect on the Agar hydrogel may be achieved by regulating the

https://doi.org/10.1021/acs.macromol.5c03189
Macromolecules 2026, 59, 1416−1428

length and number of hydrogen bonds within the Agar polymer chains.

Based on the results of rheological tests, microstructural characterizations, and the molecular dynamics simulation, the possible systematic mechanism of the Hofmeister effect on the tunability of Agar hydrogel is proposed and demonstrated in Figure 6. After the heating−cooling process, Agar polymer chains assemble into a 3D network structure via hydrogen bonds, endowing the hydrogel with insolubility in water. The abundance of H_2O molecules in the Agar hydrogel also leads to the formation of hydrogen bonds between some of the Agar polymer chains and the water molecules. The ions affect the hydrogen bonding in Agar hydrogels indirectly by altering the competition between ion−water, water−water, and polymer−water hydrogen bonds. In the salt solutions with the "salting-out" effect, ions disrupt the hydrogen bonds between Agar polymer chains and H_2O molecules in the hydration layer of the hydrogel, reducing the distance between Agar molecular chains, which is proved by the microstructural characterizations and the molecular dynamics simulation results. This "salting-out" effect promotes the aggregation of Agar polymer chains, increasing the number of hydrogen bonds between Agar polymer chains, leading to the formation of additional hydrogen-bond-based physical cross-links. As shown in Figure S9, the tensile strength decreased after H_2O immersing but recovered after reimmersion in Na_2SO_4, demonstrating that these additional cross-links strengthen the Agar hydrogels temporarily but remain reversible upon ion exchange. In the salt solutions with the "salting-in" effect, the ions disrupt the hydrogen bonds between the Agar polymer chains, increasing the hydrogen bonds formed between the Agar polymer chains and the H_2O molecules in the hydration layer of the hydrogel. This "salting-in" effect also increases the distance between the Agar polymer chains, resulting in a longer hydrogen bond length, which weakens the mechanical properties of the hydrogel. These ion-specific interactions modulate the gelation process and final network architecture, leading to tunable tensile and compressive strengths over a wide range of 54.7−412.1 kPa and 137.2−423.6 kPa, respectively. These results promote the understanding of the correlation between the cross-linking and aggregation state of polymer chains and the macroscopic properties tunability of natural polysaccharide-based single-network hydrogels, providing an innovative method for tuning their mechanical properties and microstructures.

The molecular dynamics simulation and the Hofmeister effect mechanism analysis reveal that the molecular chains of Agar hydrogels can interact with the hydration layer around them. This revelation not only offers the possibility of the water state regulation within the system via the salt solution immersion but also provides verification for elucidating the mechanism of the Hofmeister effect in Agar hydrogels from a reverse perspective.

Due to the strong hydration ability of the hydrogel, the differences in hydrogen bonds between molecules enable the classification of water within the polymer network into three states: bound water (BW), free water (FW), and intermediate water (IW), as shown in Figure 7a. Among them, FW refers to water molecules behaving as in bulk water and interacts with four adjacent water molecules via hydrogen bonding. BW is generated through the hydrophilic functional groups of Agar polymer chains capturing water molecules from FW via stronger hydrogen bonds, while water molecules next to BW interacting with fewer than four water molecules form IW.[42] Different states of water exhibit distinct thermal properties and spectroscopic features, while differential scanning calorimetry (DSC) and Raman spectroscopy are the most commonly employed and effective methods for distinguishing these water states.[43] Among them, FW shows a distinct endothermic peak near 0 °C in DSC measurements and hydrogen-bonding characteristics similar to bulk liquid water in Raman measurements. IW exhibits a broadened melting peak or a peak shifted to lower temperatures between −5 °C and −20 °C in DSC measurements and peaks shift slightly compared to bulk water in Raman measurements. BW shows no obvious melting peak in DSC due to the strong interaction between BW and polymer chains, indicating that it does not crystallize or melt within the experimental temperature range.[44]

As shown in Figure 7b, the endothermic peak observed in the DSC curve of the hydrogel primarily corresponds to the melting of IW and FW.[20] The contents of IW and FW in Agar hydrogel can be calculated based on the peak area after DSC curve fitting in this range using a Gaussian function (Figure 7c). For IW and FW, Agar/SO_4^{2-} hydrogel has the lowest IW content and the highest FW content, with values of 20.4% and 61.2%, respectively. In contrast, Agar/I^- hydrogel has the highest IW content and the lowest FW content, with values of 63.6% and 32.8%, respectively. The FW values of Agar/H_2O hydrogel and Agar/Cl^- hydrogel are similar. Since BW in the hydrogel interacts strongly with the hydrophilic chain through hydrogen bonds, its content primarily depends on the number of hydrophilic groups within the polymer network, as shown in Figure 7d. As a result, Agar hydrogels immersed in different salt solutions exhibit similar BW contents.

In addition to the DSC tests, Raman spectroscopy tests were conducted on Agar hydrogels immersed in different salt solutions. The corresponding results are shown in Figure S10. The peaks of Raman shift at 3000−3800 cm^{-1} are attributed to the O−H stretching vibration of H_2O.[45] The ratio of IW to FW (IW/FW) in Agar hydrogel can be calculated based on the peak area after Raman spectrum fitting in this range using a Gaussian function. In the Raman spectrum, the peaks at 3215 and 3375 cm^{-1} are attributed to the stretching vibration of FW with four hydrogen bonds (two protons and two lone electron pairs), while the peaks at 3481 and 3625 cm^{-1} are attributed to the stretching vibration of IW with partial or complete breakage of hydrogen bonds. The Agar/SO_4^{2-} hydrogel exhibits the lowest IW/FW ratio of 0.47, while the Agar/I^- hydrogel shows the highest IW/FW ratio of 0.82. The IW/FW ratio of the Agar/H_2O hydrogel and the Agar/Cl^- hydrogel is similar, which are both 0.74. It is noted that the IW/FW ratios obtained from DSC and Raman spectroscopy differ numerically, which mainly arises from the fundamental differences in the detection principles. Specifically, DSC quantifies water states based on thermal transitions during freezing and melting of the bulk water, while Raman spectroscopy distinguishes water states based on vibrational O−H stretching bands on a microregion of the hydrogel surface.[46] Despite the numerical difference, both methods consistently demonstrate that the IW/FW ratio follows the order $I^- > Cl^- \approx H_2O > SO_4^{2-}$, which is also consistent with the Hofmeister salting-out behavior.

These results indicate that under the influence of "salting-out" ions, the hydrogen bonds between the Agar polymer chains and the H_2O molecules are disrupted, leading to a decrease in the number of IW water molecules in the hydration

https://doi.org/10.1021/acs.macromol.5c03189
Macromolecules 2026, 59, 1416−1428

layer accordingly, which in turn lowers the IW/FW ratio. Conversely, when "salting-in" ions are present in the Agar hydrogel, the hydrogen bonds between the Agar polymer chains are weakened, resulting in the formation of a greater number of hydrogen bonds between the Agar molecules and surrounding H_2O molecules. As a result, the number of IW water molecules in the hydration layer increases, which in turn raises the IW/FW ratio. Since Cl^- has minimal impact on the Agar polymers, its effect on the IW/FW ratio is similar to that of the Agar/H_2O hydrogel. The presence of "salting-in" ions promotes an increase in the IW ratio, while "salting-out" ions lead to a higher proportion of FW in the hydrogel. These results represent another manifestation of the Hofmeister effect on the microscopic state of Agar-based natural polysaccharide hydrogels, verifying the conclusion that the water state regulation can be achieved via the Hofmeister effect on Agar hydrogels in addition to the tuning of the mechanical properties.

CONCLUSIONS

In general, this work explores the correlation between the tunability of mechanical properties and the systematic mechanism via macroscopic and microscopic characterizations and molecular dynamics simulations based on the regulation of the Hofmeister effect on Agar-based single-network hydrogels. The preforming postimmersion preparation method is necessary to obtain an intact Agar hydrogel with the presence of the salt ions. Owing to the regulation of the Hofmeister salt series, its tensile and compressive strength can be tuned between 54.7−412.1 kPa and 137.2−423.6 kPa, respectively. The mesh size, cross-linking density, microstructure images, and nanostructure analysis of Agar hydrogels indicate that the tunability of the Hofmeister effect on the Agar hydrogel is related to the aggregation state of the polymer chain. The molecular dynamics simulation on the probability distribution function reveals that this phenomenon is related to the hydrogen bonds between the Agar polymer chains and the H_2O molecules of the hydration layer. The ion solution with the "salting-out" effect promotes the aggregation of the Agar molecular chains, thereby improving the mechanical properties of the hydrogel, while the "salting-in" ions exhibit the converse properties. The Hofmeister effect on the Agar hydrogel further elucidated the regulation of IW content based on the Hofmeister salt series, which can be tuned from 20.4% to 63.6%. This work provides a possibility of the tunability of Agar-based single-network hydrogels based on the principle of the Hofmeister effect, which may inspire research on other kinds of natural polysaccharide hydrogels.

ASSOCIATED CONTENT

Supporting Information

The Supporting Information is available free of charge at https://pubs.acs.org/doi/10.1021/acs.macromol.5c03189.

The molecular dynamics simulation in the Agar molecular chain in H_2O, Na_2SO_4, NaCl and NaI salt solutions was conducted; the SEM images of the Agar/Na_2SO_4 hydrogels prepared by the preforming post-immersion method and the one-pot direct adding method; the macroscopic appearance of the Agar/H_2O and Agar/Na_2SO_4 hydrogels before and after being mechanically disrupted, heated to the sol state, and subsequently cooled to form gels again via the sol-gel transition; the tensile test of Agar hydrogels immersed in different concentrations of Na_2SO_4 solutions; rheological properties of Agar hydrogels after immersing in different ionic solutions; the pore size of Agar hydrogels after immersing in different ionic solutions; SAXS results and the corresponding fitting curve of Agar/H_2O and Agar/SO_4^{2-} hydrogels; ATR-FTIR test results of Agar hydrogels after immersing in different ionic solutions; molecular dynamics simulation process; the tensile strength of Agar/Na_2SO_4 hydrogels sequentially immersed in 1 mol L^{-1} Na_2SO_4 solution, H_2O, and then again in 1 mol L^{-1} Na_2SO_4 solution.Raman spectroscopy characterization of Agar hydrogels immersed in different ionic solutions (PDF)

AUTHOR INFORMATION

Corresponding Authors

Nam-Joon Cho − *School of Materials Science and Engineering, Nanyang Technological University, Singapore 639798, Singapore;* orcid.org/0000-0002-8692-8955; Email: njcho@ntu.edu.sg

Yu Chen − *School of Materials Science and Engineering, Beijing Institute of Technology, Beijing 100081, China; Research Center of Advanced Materials in Sports and Health and Sports & Medicine Integrative Innovation Center, Capital University of Physical Education and Sports, Beijing 100191, China*; Email: bityuchen@bit.edu.cn

Authors

Jueying Yang − *Institute of Artificial Intelligence in Sports, Capital University of Physical Education and Sports, Beijing 100191, China; School of Materials Science and Engineering, Nanyang Technological University, Singapore 639798, Singapore; School of Materials Science and Engineering, Beijing Institute of Technology, Beijing 100081, China;* orcid.org/0000-0002-3450-7083

Weiting Huang − *School of Materials Science and Engineering, Beijing Institute of Technology, Beijing 100081, China*

Jingyu Deng − *School of Materials Science and Engineering, Nanyang Technological University, Singapore 639798, Singapore*

Jian Li − *School of Materials Science and Engineering, Nanyang Technological University, Singapore 639798, Singapore*

Shahrudin Ibrahim − *School of Materials Science and Engineering, Nanyang Technological University, Singapore 639798, Singapore*

Younghwan Choe − *School of Materials Science and Engineering, Nanyang Technological University, Singapore 639798, Singapore*

Chang Su Lim − *School of Materials Science and Engineering, Nanyang Technological University, Singapore 639798, Singapore*

Lijie Li − *School of Materials Science and Engineering, Beijing Institute of Technology, Beijing 100081, China*

Complete contact information is available at: https://pubs.acs.org/10.1021/acs.macromol.5c03189

Author Contributions

The manuscript was written through contributions of all authors. All authors have given approval to the final version of the manuscript.

https://doi.org/10.1021/acs.macromol.5c03189
Macromolecules 2026, 59, 1416−1428

Notes

The authors declare no competing financial interest.

■ ACKNOWLEDGMENTS

This work was supported by the Beijing Natural Science Foundation (Grant No. L222036), Special Key Projects (Grant No. 2022-JCJQ-ZD-224-12), the Chinese Scholarship Council under Grant No. 202206030117, and the Ministry of Education in Singapore under Grant No. MOE-MOET32022-0002 and the Centre for Cross Economy, Nanyang Technological University.

■ REFERENCES

(1) Yang, J.; Chen, Y.; Zhao, L.; Zhang, J.; Luo, H. Constructions and properties of physically cross-linked hydrogels based on natural polymers. *Polym. Rev.* **2023**, *63* (3), 574−612.
(2) Yin, H.; You, M.; Yu, H.; Si, X.; Zheng, Y.; Cui, W.; Zhu, L.; Chen, Q. Rate-dependent fracture behaviors of agar-based hybrid double-network hydrogels. *Macromolecules* **2024**, *57* (9), 4024−4033.
(3) Martínez-Sanz, M.; Ström, A.; Lopez-Sanchez, P.; Knutsen, S. H.; Ballance, S.; Zobel, H. K.; Sokolova, A.; Gilbert, E. P.; López-Rubio, A. Advanced structural characterisation of agar-based hydrogels: Rheological and small angle scattering studies. *Carbohydr. Polym.* **2020**, *236*, 115655.
(4) Li, J.; Shi, Q.; Wu, X.; Li, C.; Chen, X. In vitro and in vivo evaluation of 3D biodegradable thermo/pH sensitive sol-gel reversible hydroxybutyl chitosan hydrogel. *Mater. Sci. Eng. C* **2020**, *108*, 110419.
(5) Pereira, S. G.; Martins, A. A.; Mata, T. M.; Pereira, R. N.; Teixeira, J. A.; Rocha, C. M. R. Life cycle assessment and cost analysis of innovative agar extraction technologies from red seaweeds. *Bioresour. Technol.* **2024**, *414*, 131649.
(6) Arayesh, S.; Tanhaei, B.; Khoshkho, S. M.; Shahrak, M. N.; Ayati, A.; Far, S. K. Enhanced dual-drug loaded κ-carrageenan/agar hydrogel films for wound dressing: Optimizing swelling and drug release. *Int. J. Biol. Macromol.* **2025**, *306*, 141295.
(7) Nie, Z.; Peng, K.; Lin, L.; Yang, J.; Cheng, Z.; Gan, Q.; Chen, Y.; Feng, C. A conductive hydrogel based on nature polymer agar with self-healing ability and stretchability for flexible sensors. *Chem. Eng. J.* **2023**, *454*, 139843.
(8) Yang, J.; Wang, H.; Huang, W.; Peng, K.; Shi, R.; Tian, W.; Lin, L.; Yuan, J.; Yao, W.; Ma, X.; et al. A natural polymer-based hydrogel with shape controllability and high toughness and its application to efficient osteochondral regeneration. *Mater. Horiz.* **2023**, *10* (9), 3797−3806.
(9) He, Q.; Huang, Y.; Wang, S. Hofmeister effect-assisted one step fabrication of ductile and strong gelatin hydrogels. *Adv. Funct. Mater.* **2018**, *28* (5), 1705069.
(10) Cheng, C.; Peng, X.; Xi, L.; Wan, C.; Shi, S.; Wang, Y.; Yu, X. An agar−polyvinyl alcohol hydrogel loaded with tannic acid with efficient hemostatic and antibacterial capacity for wound dressing. *Food Funct.* **2022**, *13* (18), 9622−9634.
(11) Garcia-Orue, I.; Santos-Vizcaino, E.; Uranga, J.; de la Caba, K.; Guerrero, P.; Igartua, M.; Hernandez, R. M. Agar/gelatin hydro-film containing EGF and Aloe vera for effective wound healing. *J. Mater. Chem. B* **2023**, *11* (29), 6896−6910.
(12) Yang, J.; Huang, W.; Peng, K.; Cheng, Z.; Lin, L.; Yuan, J.; Sun, Y.; Cho, N.-J.; Chen, Y. Versatile agar-zwitterion hybrid hydrogels for temperature self-sensing and electro-responsive actuation. *Adv. Funct. Mater.* **2024**, *34* (19), 2313725.
(13) Wu, S.; Hua, M.; Alsaid, Y.; Du, Y.; Ma, Y.; Zhao, Y.; Lo, C.-Y.; Wang, C.; Wu, D.; Yao, B.; et al. Poly(vinyl alcohol) hydrogels with broad-range tunable mechanical properties via the Hofmeister effect. *Adv. Mater.* **2021**, *33* (11), 2007829.
(14) Sun, X.; Mao, Y.; Yu, Z.; Yang, P.; Jiang, F. A biomimetic "salting out—alignment—locking" tactic to design strong and tough hydrogel. *Adv. Mater.* **2024**, *36* (25), 2400084.
(15) Zhang, Y.; Furyk, S.; Bergbreiter, D. E.; Cremer, P. S. Specific ion effects on the water solubility of macromolecules: PNIPAM and the Hofmeister series. *J. Am. Chem. Soc.* **2005**, *127* (41), 14505−14510.
(16) Roy, S.; Javid, N.; Frederix, P. W.; Lamprou, D. A.; Urquhart, A. J.; Hunt, N. T.; Halling, P. J.; Ulijn, R. V. Dramatic specific-ion effect in supramolecular hydrogels. *Chemistry* **2012**, *18* (37), 11723−11731.
(17) Jaspers, M.; Rowan, A. E.; Kouwer, P. H. J. Tuning hydrogel mechanics using the Hofmeister effect. *Adv. Funct. Mater.* **2015**, *25* (41), 6503−6510.
(18) Jin, Y.; Lu, S.; Chen, X.; Fang, Q.; Guan, X.; Qin, L.; Chen, C.; Zhao, C. Time-salt type superposition and salt processing of poly(methacrylamide) hydrogel based on Hofmeister series. *Macromolecules* **2024**, *57* (6), 2746−2755.
(19) Huang, S.; Hou, L.; Li, T.; Jiao, Y.; Wu, P. Antifreezing hydrogel electrolyte with ternary hydrogen bonding for high-performance zinc-ion batteries. *Adv. Mater.* **2022**, *34* (14), 2110140.
(20) Ren, J.; Chen, L.; Gong, J.; Qu, J.; Niu, R. Hofmeister effect mediated hydrogel evaporator for simultaneous solar evaporation and thermoelectric power generation. *Chem. Eng. J.* **2023**, *458*, 141511.
(21) Wu, Y.; Mu, Y.; Luo, Y.; Menon, C.; Zhou, Z.; Chu, P. K.; Feng, S. P. Hofmeister effect and electrostatic interaction enhanced ionic conductive organohydrogels for electronic applications. *Adv. Funct. Mater.* **2022**, *32* (15), 2110859.
(22) Yin, J.; Jia, P.; Ren, Z.; Zhang, Q.; Lu, W.; Yao, Q.; Deng, M.; Zhou, X.; Gao, Y.; Liu, N. Recent advances in self-powered sensors based on ionic hydrogels. *Research* **2025**, *8*, 0571.
(23) Li, J.; Chee, H. L.; Chong, Y. T.; Chan, B. Q. Y.; Xue, K.; Lim, P. C.; Loh, X. J.; Wang, F. Hofmeister effect mediated strong PHEMA-gelatin hydrogel actuator. *ACS Appl. Mater. Interfaces* **2022**, *14* (20), 23826−23838.
(24) Das, S.; Majumdar, S. Enhancing the properties of self-healing gelatin alginate hydrogels by Hofmeister mediated electrostatic effect. *ChemPhysChem* **2024**, *25* (1), No. e202300660.
(25) Rotjanasuworapong, K.; Thummarungsan, N.; Lerdwijitjarud, W.; Sirivat, A. Facile formation of agarose hydrogel and electro-mechanical responses as electro-responsive hydrogel materials in actuator applications. *Carbohydr. Polym.* **2020**, *247*, 116709.
(26) Hou, W.; Sheng, N.; Zhang, X.; Luan, Z.; Qi, P.; Lin, M.; Tan, Y.; Xia, Y.; Li, Y.; Sui, K. Design of injectable agar/NaCl/polyacrylamide ionic hydrogels for high performance strain sensors. *Carbohydr. Polym.* **2019**, *211*, 322−328.
(27) Xu, L.; Chen, Y.; Guo, Z.; Tang, Z.; Luo, Y.; Xie, S.; Li, N.; Xu, J. Flexible Li+/agar/pHEAA double-network conductive hydrogels with self-adhesive and self-repairing properties as strain sensors for human motion monitoring. *React. Funct. Polym.* **2021**, *168*, 105054.
(28) Wu, S.; Zhu, C.; He, Z.; Xue, H.; Fan, Q.; Song, Y.; Francisco, J. S.; Zeng, X. C.; Wang, J. Ion-specific ice recrystallization provides a facile approach for the fabrication of porous materials. *Nat. Commun.* **2017**, *8* (1), 15154.
(29) Zhu, F.; Feng, S.; Wang, Z.; Zuo, Z.; Zhu, S.; Yu, W.; Ye, Y. N.; An, M.; Qian, J.; Wu, Z. L.; et al. Co-ion specific effect aided phase separation in polyelectrolyte hydrogels toward extreme strengthening and toughening. *Macromolecules* **2023**, *56* (15), 5881−5890.
(30) Wei, W. Hofmeister effects shine in nanoscience. *Adv. Sci.* **2023**, *10* (22), No. e2302057.
(31) Liu, G.; Ma, Q.; Zhang, X. Agar-polyacrylamide dual network hydrogel-carbon nanotube composites with long-term stability for high efficient solar water purification. *Compos. Commun.* **2025**, *53*, 102248.
(32) Behera, L.; Mohapatra, S. A stretchable PVA−agar hydrogel patch embedded with metal-doped carbon dots (MCD) for monitoring the Ca^{2+} biomarker. *Mater. Adv.* **2025**, *6* (4), 1392−1402.
(33) Polat, T. G.; Duman, O.; Tunç, S. Agar/κ-carrageenan/montmorillonite nanocomposite hydrogels for wound dressing applications. *Int. J. Biol. Macromol.* **2020**, *164*, 4591−4602.

https://doi.org/10.1021/acs.macromol.5c03189
Macromolecules 2026, 59, 1416−1428

(34) Sacco, P.; Piazza, F.; Marsich, E.; Abrami, M.; Grassi, M.; Donati, I. Ionic strength impacts the physical properties of agarose hydrogels. *Gels* **2024**, *10* (2), 94.
(35) Yang, J.; Chen, Y.; Zhao, L.; Feng, Z.; Peng, K.; Wei, A.; Wang, Y.; Tong, Z.; Cheng, B. Preparation of a chitosan/carboxymethyl chitosan/AgNPs polyelectrolyte composite physical hydrogel with self-healing ability, antibacterial properties, and good biosafety simultaneously, and its application as a wound dressing. *Composites, Part B* **2020**, *197*, 108139.
(36) Fermino, T. Z.; Awano, C. M.; Moreno, L. X.; Vollet, D. R.; de Vicente, F. S. Structure and thermal stability in hydrophobic Pluronic F127-modified silica aerogels. *Microporous Mesoporous Mater.* **2018**, *267*, 242−248.
(37) Deng, J.; Zhao, Z.; Yeo, X. Y.; Yang, C.; Yang, J.; Ferhan, A. R.; Jin, B.; Oh, C.; Jung, S.; Suresh, S.; et al. Plant-based shape memory cryogel for hemorrhage control. *Adv. Mater.* **2024**, *36* (36), 2311684.
(38) He, Q.; Qiao, Y.; Medina Jimenez, C.; Hackler, R.; Martinson, A. B. F.; Chen, W.; Tirrell, M. V. Ion specificity influences on the structure of zwitterionic brushes. *Macromolecules* **2023**, *56* (5), 1945−1953.
(39) Huang, L.; Jin, S.; Bao, F.; Tang, S.; Yang, J.; Peng, K.; Chen, Y. Construction of a physically cross-linked carrageenan/chitosan/calcium ion double-network hydrogel for 3-Nitro-1, 2, 4-triazole-5-one removal. *J. Hazard. Mater.* **2022**, *424*, 127510.
(40) Ge, W.; Cao, S.; Yang, Y.; Rojas, O. J.; Wang, X. Nanocellulose/LiCl systems enable conductive and stretchable electrolyte hydrogels with tolerance to dehydration and extreme cold conditions. *Chem. Eng. J.* **2021**, *408*, 127306.
(41) Bruce, E. E.; Okur, H. I.; Stegmaier, S.; Drexler, C. I.; Rogers, B. A.; van der Vegt, N. F. A.; Roke, S.; Cremer, P. S. Molecular mechanism for the interactions of hofmeister cations with macromolecules in aqueous solution. *J. Am. Chem. Soc.* **2020**, *142* (45), 19094−19100.
(42) Zhao, F.; Guo, Y.; Zhou, X.; Shi, W.; Yu, G. Materials for solar-powered water evaporation. *Nat. Rev. Mater.* **2020**, *5* (5), 388−401.
(43) Guo, Y.; Bae, J.; Fang, Z.; Li, P.; Zhao, F.; Yu, G. Hydrogels and hydrogel-derived materials for energy and water sustainability. *Chem. Rev.* **2020**, *120* (15), 7642−7707.
(44) Gun'ko, V. M.; Savina, I. N.; Mikhalovsky, S. V. Properties of water bound in hydrogels. *Gels* **2017**, *3* (4), 37.
(45) Sun, M.; Wang, X.; Yu, Y.; Li, M.; Wang, M.; Zhang, W.; Yang, Z.; Zhou, J.; Yang, H.; Wang, C. Ultra-efficient, anisotropic cellulose aerogel with polydopamine interfacial bridged structure and photothermal modification for seawater desalination. *Research* **2025**, *8*, 0888.
(46) Zou, H.; Meng, X.; Zhao, X.; Qiu, J. Hofmeister Effect-Enhanced Hydration Chemistry of Hydrogel for High-Efficiency Solar-Driven Interfacial Desalination. *Adv. Mater.* **2023**, *35* (5), 2207262.

https://doi.org/10.1021/acs.macromol.5c03189
Macromolecules 2026, 59, 1416−1428